

# Computational study of structural dependence of catalytic properties of Pt-Ru nanoalloy catalysts

B. Prasai\* and V. Petkov\*

\* Department of Physics, Central Michigan University, Mt. Pleasant, MI 48858

## ABSTRACT

3D structure models of Pt-Ru alloy nanoparticles (NPs) are built by molecular dynamics simulations. Models are refined against the experimental PDF data by reverse Monte Carlo simulations and analysed in terms of prime structural characteristics such as metal-to-metal bond lengths and first coordination numbers for Pt and Ru atoms. Structural characteristics of activated NPs and data for their catalytic activity are compared side by side and strong evidence is found that electronic effects, indicated by significant changes in Pt-Pt and Ru-Ru metal bond lengths at NP surface, and practically unrecognized so far atomic ensemble effects, indicated by the prevalence of particular configurations of Pt and Ru atoms at NP surface and distinctive packing of atomic layers near NP surface, contribute to the observed enhancement of the catalytic activity of composition about 50:50. Implications of so-established relationships between the atomic structure and catalytic activity of Pt-Ru alloy NPs on efforts aimed at improving further the latter by tuning-up the former are discussed and the usefulness of detailed NP structure studies to advancing science and technology of metallic NPs explored for catalytic applications is exemplified.

**Keywords:** nanoparticle structure modeling, molecular dynamics, fuel cell, Catalysis, sutton-chen, reverse Monte Carlo.

## 1 INTRODUCTION

In the recent years, metallic nanoparticles (NPs) are being extensively explored for their practical use in various applications such as catalysis, photonics, magnetic storage media, and drug delivery[1, 2, 3, 4]. The exploration of the metallic NPs as catalytic agents has boomed because of their use in fuel cell technologies based on catalysis. Metal nanoalloys, a few nanometer in size, based on Noble metals have shown a great promise as catalyst for several technologically important reactions. Here we explored Pt-Ru nanoalloys which is one of the many important nanoalloy catalysts. Pt-Ru was chosen because of its importance for the development of highly pursued current devices for clean energy conversion such as fuel cells, particularly for its remark-

able ability to speed up gas-phase CO oxidation and ethanol electro-oxidation reactions. Since most of the studies on Pt-Ru nanoalloys are focused on their catalytic properties with a limited knowledge of the atomic structure, here we pay particular attention on determining the atomic structure of these nanoalloys in fine detail and hence establishing the correlations between atomic structure and catalytic properties, with a hope that, once known, these correlations can provide a feedback loop for streamlining synthesis and optimization of Pt-Ru nanoalloys for fuel cells related applications.

For the purpose we built 3D structure models for catalytically active  $Pt_xRu_{100-x}$ ; ( $x=31, 49$  and  $75$ ) alloy NPs by Molecular Dynamics (MD) simulations and further refined by reverse Monte Carlo (RMC) simulations guided by the experimental atomic pair distribution functions (PDFs). RMC refined models are then analyzed in terms of structural characteristics important for catalysis such as NP phase state, distribution of first atomic neighbor distances, i.e. metal-to-metal bond lengths and first atomic coordination numbers paying particular attention to Pt and Ru atoms at NP surface since it is the NP surface where catalytic reactions take place, and correlated data for catalytic activity with structural characteristics of respective NPs and showed the usefulness of so-established relationships between the atomic structure and catalytic activity of Pt-Ru alloy NPs to efforts aimed at improving further the latter by tuning up the former.

## 2 COMPUTATIONAL METHODS

MD simulations were carried out with the help of computer program DL-POLY [5] under canonical NVT ensemble in the absence of periodic boundary conditions. Velocity Verlet algorithm with a time step of 2 fs was used. Initial model atomic configurations were equilibrated for 200 ps at 700K, which is just about the temperature at which Pt-Ru NPs were post-synthesis treated as to be activated for catalytic applications. The models were then cooled down to room temperature in steps of 50K and again equilibrated for 100 ps. Sutton-Chen potential parameters used in this study are taken from Ref. [6]. Reverse Monte Carlo (RMC) simulations, details of which are given in Ref.[6], were used to further

refine MD generated structure models for Pt-Ru NPs.

### 3 RESULTS AND DISCUSSION

Accounting for the findings of simplistic empirical modeling, 3D models of post-synthesis treated (catalytically active) Pt-Ru alloy NPs were built by MD simulations based on the archetypal for current metal and alloy atomic structure theory Sutton-Chen (SC) method. MD models featured NPs with the chemical composition, chemical pattern, size ( $\sim 4.5$  nm) and shape (spherical) of actual Pt-Ru alloy NPs studied here as previously explained in Ref.[6]. Resulted 3D models are shown in Figure 1a and the atomic PDFs derived from the models are compared with the respective experimental PDFs in Figure 2a. As can be seen in Figure 2a, MD built structure models produce atomic PDFs that capture the essence of experimental ones but fail in reproducing them in fine detail. In particular, MD models fail in reproducing the position, broadening and intensity of several peaks in the experimental PDFs, i.e. the radii, degree of atomic positional disorder and atomic population of several coordination spheres in Pt-Ru alloy NPs. The inability of MD models to reproduce accurately the radii of atomic coordination spheres in  $\text{Pt}_x\text{Ru}_{100-x}$  alloy NPs may be expected since SC method employed by MD is, like most theoretical methods currently in use, validated against experimental data for the lattice parameters of respective solids. Results of empirical modeling carried out here, however, showed clearly that NP “lattice parameters”, i.e. the characteristic interatomic distances in Pt-Ru alloy NPs, are different from these of the respective solids. Indeed this is a rather common observation since interatomic distances in metallic NPs can get compressed or stretched out considerably and non uniformly as a result of the inherently increased surface tension of NPs[7] and/or NP surface environment effects such as, for example, exposure to reactive (e.g.  $\text{H}_2$ ) gases [8]. Such an effect is atypical for the respective solids. Besides, charge transfer and optimization of atomic-level stresses in metallic alloy NPs can result in a considerable change in the radii/size of metallic species involved which, again, may not be the case with the respective solids[9, 10]. The inability of MD models to reproduce accurately the degree of local structural disorder in Pt-Ru alloy NPs, in particular its inherent enhancement in coordination spheres involving atoms close to/at the extended NP surface, may also be expected. It is due to the fact that MD treats all atoms in structure models alike whereas atoms inside and at the surface of real-world metallic NPs are not necessarily alike in respect to their immediate atomic neighborhood, and others. The inability of MD models to reproduce accurately the distribution of Pt and Ru atoms across NPs is not a big surprise either. Nevertheless, as discussed in Ref.[9], MD simulations are useful in providing plausible struc-

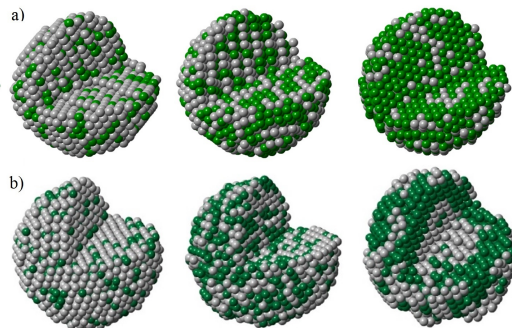


Figure 1: a) MD generated 3D structure models of  $\text{Pt}_x\text{Ru}_{100-x}$  alloy NPs ( $x=75$ , left); ( $x=49$ , middle); ( $x=31$ , right), b) RMC refined 3D structure models with the corresponding compositions. The non-uniform distribution of Pt in  $\text{Pt}_{31}\text{Ru}_{69}$  indicates a clear segregation of Pt species at the center and surface of NPs leading to an onion-like chemical pattern. Ru atoms are in green and Pt in gray.

ture models for metallic NPs that can be refined further, when necessary.

MD models were refined further by RMC simulations. In the simulations positions of atoms in MD models of Figure 1a were adjusted, including switching the positions of nearby Pt and Ru atoms, as that the difference between RMC model derived and respective experimental PDF data is reduced as much as possible. At the same time model’s energy was minimized, i.e. model’s stability maximized, to the fullest possible extent using reliable pair-wise (Lennard-Jones type) potentials. RMC refined models for Pt-Ru nanoalloys are shown in Figure 1b and the atomic PDFs derived from the corresponding models are compared with the respective experimental PDFs in Figure 2b. As can be seen in Figure 2b, atomic PDFs derived from RMC refined 3D structure models for Pt-Ru alloy NPs reproduce respective experimental atomic PDFs in very good detail (see the reported  $R_w$  factors), including the region of higher  $r$ -values which is sensitive to structural features of NP surface. Precise accounting for the latter is important for catalysis since it is the NP surface where catalytic reactions take place.

With 3D models of realistic size, shape, chemical composition, chemical species ordering pattern, type of atomic ordering and atomic coordination spheres, including coordination radii and numbers, tuned up against relevant experimental PDF data at hand all important structural characteristics of actual metallic NPs studied can be derived. Here we concentrate on structural characteristics relevant to catalytic properties of metallic NPs such as metal-to-metal bond lengths and coordination numbers (CNs) paying particular attention to metallic species at NP surface. First neighbor Pt-Pt and

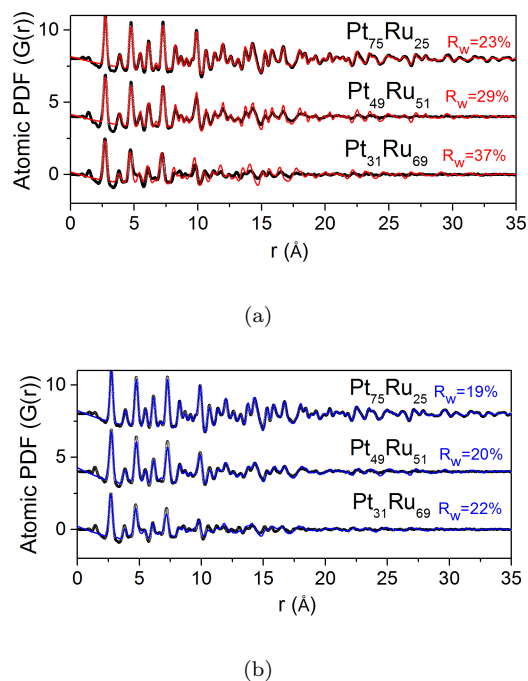


Figure 2: a) Experimental (symbols) and model (lines in red) PDFs for MD generated  $Pt_xRu_{100-x}$  alloy NP ( $x=31, 49$  and  $75$ ) atomic configurations, shown in Figure 1a. b) Experimental (symbols) and model (lines in blue) PDFs for RMC refined respective Pt-Ru alloy NP atomic configurations, shown in Figure 1b. Model's quality indicators,  $R_w$  are shown for each data set.

Ru-Ru distances, i.e. metal-to-metal bond lengths, and first Pt-Pt and Pt-Ru CNs for Pt and Ru atoms at the surface of the Pt-Ru alloy NPs, as derived from their 3D structure models of Figure 1b, are shown in Figure 3. Experimental data for the catalytic activity of same NPs for gas-phase oxidation of CO and electro-oxidation of ethanol, obtained as described in Ref.[6], are also shown in the Figure. Inspection of so-summarized NP atomic structure vs NP property data indicates that the catalytic activity of Pt-Ru alloy NPs studied here peaks when i) Pt-Pt and Ru-Ru bond lengths at NP surface are, respectively, shortened and elongated most and ii) surface Pt-Pt and Pt-Ru first CNs are nearly identical. To comprehend the observed NP atomic structure-catalytic activity relationships we reasoned them within the framework of three most frequently evoked explanations for the higher catalytic activity of metallic alloy NPs as compared to that of respective monometallic NPs. Those explanations argue that i) different metallic species at the surface of alloy NPs do not interact but act cooperatively as to promote particular steps of chemical reactions, ii) different metallic species at the surface of alloy NPs interact by exchanging charge and/or adjusting size both affecting their electronic structure in a way favorable for chemical reactions and iii) different

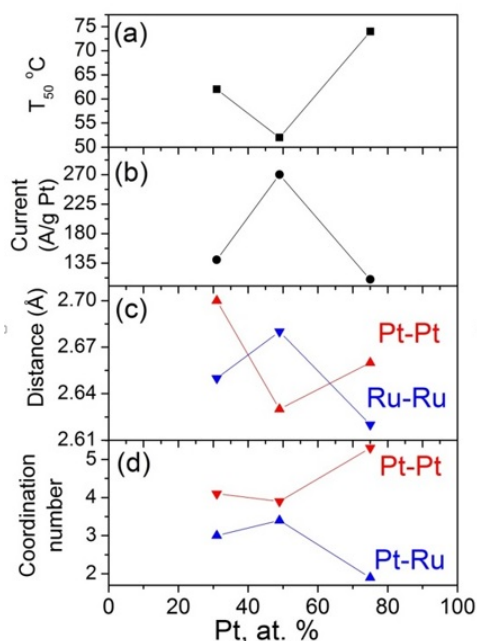


Figure 3: a) Catalytic activity of post-synthesis treated  $Pt_xRu_{100-x}$  alloy NPs ( $x=31, 49$  and  $75$ ) for gas-phase oxidation of CO given in terms of the temperature  $T_{50}$  at which 50 % conversion of CO is achieved, b) Catalytic activity of respective Pt-Ru alloy NPs for electro-oxidation of ethanol given in terms of peak current generated as a result of the reaction, c) Pt-Pt and Ru-Ru bond lengths at the surface of RMC refined 3D atomic structures of  $Pt_xRu_{100-x}$  alloy NPs ( $x=31, 49$  and  $75$ ) and d) first neighbor Pt-Pt and Pt-Ru CNs at the surface of same NPs.

metallic species at NP surface assemble in particular configurations providing active catalytic sites[11, 12].

In the case of Pt-Ru alloy NPs explanation (i) has been put forward in terms of the so-called bi-functional mechanism[13] envisioning formation of surface Ru-hydrate species easing CO oxidation on nearby surface Pt atoms. The mechanism, however, has been found incapable of explaining the improved catalytic activity of Pt-Ru NPs wherein Pt atoms completely cover NP surface thus screening all Ru atoms from chemical species adsorbed at that surface. On the other hand, explanation (ii) has found strong support in numerous experimental and theoretical studies on Pt-Ru alloy NPs indicating the presence of charge transfer between Pt and Ru species[16, 17] accompanied by a considerable shortening of Pt-Pt and elongation of Ru-Ru metal bond lengths[11, 12, 18]. According to Pauling's theory of chemical bonds [19, 20] some charge transfer between Pt and Ru species may be expected due to their somewhat different electronegativity that is 2.3 and 2.2, respectively. Change in Pt-Pt

## REFERENCES

and Ru-Ru bond lengths may also be expected since in order for the atomic-level stresses in Pt-Ru alloy NPs to be optimized the larger in size Pt species (2.77 Å) should shrink and the smaller in size Ru species (2.67 Å) expand as that the ratio of their size/radii becomes as close to one as possible [20, 21]. Changes in metal-to-metal bond length, strength and the electronic structure of respective metal species are known to be largely interrelated[20, 21] and so difficult to take apart. Nevertheless, it has been shown that metal-to-metal bond length changes of the type shown in Figure 3c would induce a strong downshift of the d electron states of surface Pt atoms in  $Pt_xRu_{100-x}$  alloy NPs at  $x \sim 50$ . This would modify the energies of bonding of chemical species to surface Pt atoms and so the activation barriers of critical steps of chemical reactions, such as gas-phase oxidation of CO and electro-oxidation of ethanol, in a way enhancing the catalytic activity of Pt-Ru alloy NPs for  $x \sim 50$ [11, 12, 18]. Indeed this is exactly what data in Figure 3(a and b) show. Explanation (iii) has been contemplated in several studies on Pt-Ru alloy NPs [11, 22, 23] but not recognized explicitly so far. Data in Figure 3 provides strong evidence that not only electronic (ii) but also atomic ensemble (iii) effects, signified by the prevalence of atomic configurations where both Pt and Ru metal species have pretty much the same number of unlike first neighbors (Pt-Pt and Pt-Ru first CNs of 3.8 and 3.5, and Ru-Pt and Ru-Ru CNs of 3.5 and 3.8, respectively[6]), contribute to the enhanced catalytic activity for  $x \sim 50$ .

## 4 CONCLUSION

Catalytic activity of metallic NPs is governed by a series of destruction and creation of bonds between NP surface atoms and chemical species adsorbed at NP surface. Complete or partial alloying of metal species at the nanoscale can modify the electronic structure, hence, size (or vice versa) and arrangement of individual metallic species at NP surface thus influencing the catalytic activity of metallic NPs significantly. The arrangement, size, and electronic structure of atoms at NP surface, however, strongly depend on the way atoms in the layer(s) beneath it are positioned. Therefore, detailed knowledge of the atomic-scale structure across metallic alloy NPs is a prerequisite to achieving a better understanding of their catalytic properties and, hence, enabling a rational design approach to producing and optimizing metallic alloy NPs for catalytic applications.

## 5 ACKNOWLEDGMENTS

Work on this paper was supported by DOE-BES Grant DE-SC0006877.

- [1] J. K. Norskov and C. H. Christensen, *Science*, 312, 1322, 2006.
- [2] S. Link, Z. L. Wang and M. A. El-Sayed, *J. Phys. Chem.*, 103, 3529, 1999.
- [3] D. Alloyeau, C. Ricolleau, C. Mottet, T. Oitkawa, C. Langlois, L. Y. Bouar, N. Braidy and A. Loiseau, *Nature Mater.*, 8, 940, 2009.
- [4] P. Tartaj, M. d. P. Morales, S. Veintemillas-Verdaguer, T. Gonzalez-Carreno and C. J. Serna, *J. Phys. D: Appl. Phys.*, 36, R182, 2003.
- [5] W. Smith, W. C. Yong and P. M. Rodger, *Molecular Simulation*, 28, 86, 2002.
- [6] B. Prasai, Y. Ren, S. Shan, Y. Zhao, H. Cronk, J. Luo, C.-J. Zhong and V. Petkov, *Nanoscale* [in Press].
- [7] W. J. Huang, R. Sun, J. Tao, L. D. Menard, R. G. Nuzzo and J. M. Zuo, *Nature Mater.*, 7, 308, 2008.
- [8] V. Petkov, S. Shan, P. Chupas, J. Yin, L. Yang, J. Luo and C. J. Zhong *Nanoscale*, 5, 7379, 2013.
- [9] V. Petkov, B. Prasai, Y. Ren, S. Shan, J. Luo, P. Joseph and C. J. Zhong *Nanoscale*, 6, 10048, 2014.
- [10] V. Petkov, S. Shastri, S. Shan, P. Joseph, J. Luo, C. J. Zhong, T. Nakamura, Y. Herbanli and S. Sato, *J. Phys. Chem. C*, 117, 22131, 2013.
- [11] B. Hammer and J. K. Norskov, *Adv. In Catalysis*, 45, 71, 2007.
- [12] J. K. Norskov, T. Biggaard, J. Rossmeisl and C. H. Christiansen, *Nat. Chemistry*, 1, 3746, 2009.
- [13] H. A. Gaisteiger, N. Markovic, P. N. Ross, E. J. Cairns, *J. Phys. Chem.*, 98, 617, 1994.
- [14] L. Zhang, J. Kim, H. M. Cheng, F. Nah, K. Dudeck, Ru-Shi liu, G. A. Botton and J. Zhang, *J. Power. Sources*, 196 9117, 2011.
- [15] S. Alayoglu, A. U. Nilekar, M. Mavrikakis, B. Eichhorn. *Nature Materials*, 7 (4) 333, 2008.
- [16] J. McBreen and S. Mukerjee, *J. Electrochem. Soc.*, 142, 3399, 1995.
- [17] P. Hu, D. King, M.H. Lee and M.C. Payne, *Chem. Phys. Lett.*, 246, 73, 1995.
- [18] A. Schlapka, M. Liska, A. Gros, U. Kasberger and P. Jacob, *Phys. Rev. Lett.*, 91, 016101, 2003.
- [19] L. Pauling, Ithaca, NY: Cornell University Press., 1975.
- [20] L. Pauling, *Proc. Natl. Acad. Sci. U. S. A.*, 84, 4754, 1987.
- [21] Rajasekharam, T.; Seshubai, V., *Acta Crystallogr. Sect. A*, 68, 156, 2012.
- [22] L. Giorgi, A. Pozio, C. Bracchhini, R. Giori and S. Turtu, *J. Appl. Electrochem.*, 31, 325, 2001.
- [23] S. Stoupin, E-H. Chung, S. Chattopadhyay, C. U. Segre and E. S. Smotkin, *J. Phys. Chem. B.*, 110, 9932, 2006.
- [24] C. Bock, B. MacDougall and Y. LePag, *J. Electrochem. Soc.*, 151, A1269, 2004.